Properties of the Neutron

Konstantin Protasov
Laboratory for Subatomic Physics and Cosmology,
University Grenoble-Alpes, CNRS/IN2P3
53 rue des Martyrs, 38026 Grenoble, France

Abstract

In this lecture, we present a brief description of properties of the neutron. We describe its internal properties: life time, mass, charge, magnetic and electric dipole moments… Particular attention will be paid to two most important characteristics of the neutron – its life time and electric dipole moment – both of them are now studied in a few different experiments. Moreover, the measurement of the neutron life time is a subject to discussion within the scientific community because the last result published very recently is in contradiction with previous results.

The second part of the lecture illustrates how this "elementary" particle can be used as a tool to study different quantum systems and different interactions. The neutron is one of rare elementary particles which is successfully used in studies of all types of known interactions (strong, electromagnetic, weak, and gravitational) as well as even in searches for new unknown interactions and "new physics". As an illustration, we consider an example of "neutron whispering gallery" – an unexpected phenomenon discovered recently and which has common origins with rainbow phenomenon well known in usual optics.

Table of contents

1. Introduction

The aim of these lectures is to give a quite personal vision of some fundamental properties and the role of the neutron in physics. Each property of the neutron (charge, mass, magnetic moment, electric moment, form factors, life time, etc.) could be a subject of a separate lecture. We do not pretend to give exhaustive presentation of all these properties and physical domains where these properties are important. We prefer to give some particular illustrations and examples covering "classical" experiments which continue to be of important scientific interest (measurement of neutron life time and its electrical dipole moment) as well as very "modern" ones (whispering gallery phenomenon very well-known in physics but discovered in neutron physics only a few years ago) to show that the physics with neutron is a physics in perpetual motion.

There is another "nonscientific" point which seems to be important now. In a few years (ten or a little bit more), the scientific community doing so called neutron physics will live a transition from reactor to spallation source experiments. Historically, the most important and interesting experiments was done in the neutron reactor experiments which were used as a source of neutrons. A few reactors were constructed exclusively to do this physics, without any use of energy produced in these reactors. Today, these reactors approach the end of their life. The nowadays society hardly accepts the use of the reactors as a scientific tool and push to find an alternative. Such an alternative (not completely equivalent) is expected to be given by different spallation sources already constructed, under construction or in project. Taking into account the very high price of these sources their number in the World will be very limited and they will not obligatory located at the same place where actual scientific reactors are working. An important challenge would be to conserve this neutron community and the best way to di it is to propose new fascinating experiments with neutrons.

Neutron plays a quite particular role in physics – it is a very "multifaceted" particle. Its electrical neutrality and a long life time make this particle an excellent laboratory and a fantastical tool to investigate and to measure different physical phenomena. Together with proton, neutron composes different nuclei and it is a source of our knowledge of strong interaction. Its electrical neutrality does not mean at all that the neutron has no electromagnetic interactions: neutron being a system composed by charged quarks manifests a series of physical electromagnetic properties. Measurement of neutron magnetic moment, its electric and magnetic form factors allows us to extract precious information about its internal structure. Moreover, there is another important electromagnetic parameter describing neutron – its anomalous electric moment (which is expected to be very small within the Standard Model). Measurement of this electric moment continues since more than a half of century and already allowed to withdraw an extremely long list of hypothetical theories. We will devote a special chapter of these lectures to this physical phenomenon.

As we said neutron is a rare elementary particle which manifests experimentally all four known interactions (strong, weak, electromagnetic, and gravitational). Moreover, since a few years, in a series of articles old neutron experiments were reanalyzed and even some new experiments were done to search for other possible hypothetical interaction. These experiments are conventionally called experiments to search for the 5^{th} force. General idea is quite simple: the analytical form of known interactions is supposed to be well-known. It is particularly true for electromagnetic and gravitational interaction. In the last case, for instance, $1/r$-dependence of the interaction potential is considered as a general property of all bodies. Any deviation from these known dependencies would be a sign of "new physics".

We will devote a significant part of our presentation to these new quantum mechanical systems discovered and studies since a few decades.

2. Ultra cold neutrons

Historically, the most usual way to produce neutrons for different experiments is high flux nuclear reactor. Nuclear reactor offers a wide neutron spectrum and one needs "only" to choose the energy suitable for a given experiment. An important part of this nuclear reactor neutron spectrum is a usual Maxwell distribution. The neutron velocity in the maximum of this distribution is slightly higher than 2 km/s and the spectrum drops down rapidly for small velocities. In the most of experiments studying fundamental interactions, we are interested in neutrons of small or even extremely small energy neutrons which are called ultra cold neutrons (UCN) [1,2]. These neutrons were obtained more than 50years ago [3,4] and can be stored in mechanical or magnetic bottles for a quite long period (up to the neutron life time).

These neutrons have very small velocities, of the order of 10 m/s and their de Broglie wave length is extremely big, of the order of 1000 $\overset{o}{A}$. When such a neutron interacts with the matter bulk it cannot "see" an individual atom but a whole ensemble of atoms. This interaction with matter is described in terms of phenomenological Fermi potential. For the medium of the same chemical element atoms, the Fermi potential U is defined as

$$U = \frac{2\pi\hbar^2}{m} b_{\mathrm{coh}} N \,. \tag{1.1}$$

In this expression, b_{coh} is so-called coherent scattering length representing a microscopic parameter describing the interaction between neutron and the nucleus. N is a concentration of atoms and m is neutron mass. The sign of the potential depends on sign of b_{coh}: materials with positive scattering length or with positive Fermi potential would reflect UCN.

The phenomenon of the reflection is quite simple. Neutron motion along the z-axis perpendicular to the surface situated et $z = 0$ can be described by Schrödinger equation:

$$\frac{\hbar^2}{2m}\frac{d^2\psi(z)}{d^2 z} + (E - V(z))\psi(z) = 0 \tag{1.2}$$

with the potential

$$V(z) = \begin{cases} 0, & z < 0 \\ U, & z > 0 \end{cases}. \tag{1.3}$$

If the kinetic energy is smaller than $U > 0$, the neutron is reflected by the bulk for any incident angle. This condition of total reflection can be formulated in terms of critical velocity:

$$v_{\mathrm{lim}} = \sqrt{2mU} \,. \tag{1.4}$$

All neutrons with velocities smaller than critical one will be reflected and can be, in principle, stored in a volume. The same phenomenon of reflection is used to guide even more energetic neutrons from the reactor core to a place of experiment.

In Table 1, numerical values of critical velocities are given for some materials commonly used in this physics. For most of materials discussed here, neither inelastic scattering (due to phonon excitation) nor absorption (due to inelastic nuclear reactions) is important. Thus the UCN interaction with the material surface can be considered as purely elastic scattering, in other words, UCN cannot be "heated" by the surface which could be at sufficiently higher temperature that the temperature associated to UCN (a few mK).

Table 1. Critical velocities for different materials

Material	b_{coh}, fm	Density, g/cm^3	v_{lim} , m/s
D_2 (liquid)	13	0.15	3.82
D_2O	18.8	1.1	5.57
C (graphite)	6.65	2.25	6.11
C (diamond)	6.65	3.52	7.65
Al_2O_3	24,2	3.7	5.13
SiO_2	15.8	2.3	4.26
Steel	8.6	8.03	6.0

It is necessary to emphasize that the relative number of UCN in the reactor is extremely small. A simple estimation of their relative number for room temperature and for critical velocity corresponding to copper gives a value of $\sim 10^{-11}$. An increasing of this number is one of main challenges for experimentalists.
The first and the most direct way to do it consists in a cooling of a part of moderator in nuclear reactor. This cooling can significantly increase the lower part of Maxwell's spectrum. It could be done by introduction of so called cold source – a volume filled by liquid deuterium maintained at very small temperature (~ 25 K) close to the nuclear reactor core. The neutrons are then extracted from this volume through special neutron guide. Some new projects under development are using even deuterium ice. These systems are very efficient but need quite important cooling power.
Thermal cooling is not the only way to decrease neutron velocity. For quite small velocities, one can use gravitational field. If one makes an UCN upward extraction from the neutron source, neutrons lose a part of their energy and their velocity in gravitational field. One can also use a mechanical deceleration in a turbine where neutrons lose a part of the velocity in elastic scattering with blades of the turbine turning in sense of neutron motion.

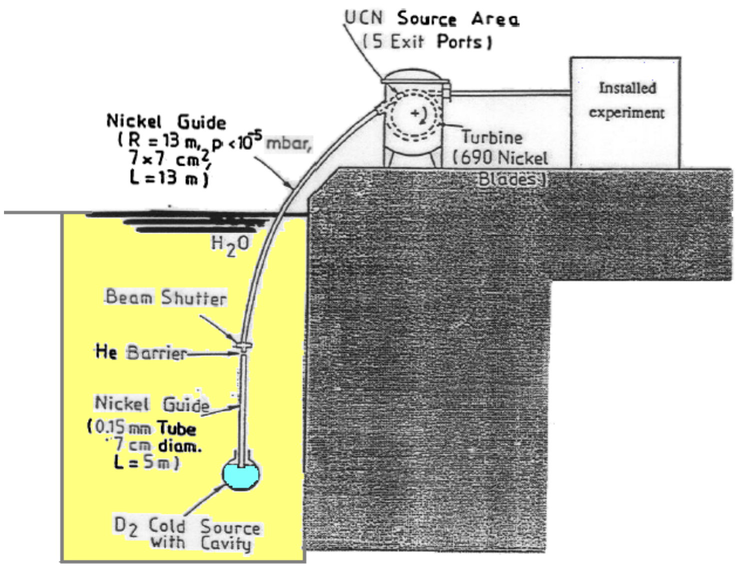

Fig. 1.2. The principal scheme of the PF1B neutron guide at the ILL

All these technics are used in the reactor of the Institute of Laue Langevin in Grenoble, which is today the reactor with the highest neutron flux in the world. Its scheme is presented in figure 1.2. The cold source of liquid deuterium is situated in a 0.7 m far from the reactor core. The neutron upward extraction is done by a slightly curved neutron guide who brings them to the turbine which allows to slow down the neutrons and to distribute them to different experimental installations.

Let us mention here another very elegant idea to produce UCN, proposed by R. Golub and M. Pandlebury [5] in 70'th and which is applied now in different experiments. This idea uses particular properties of liquid helium in its superfluid phase (helium-II).

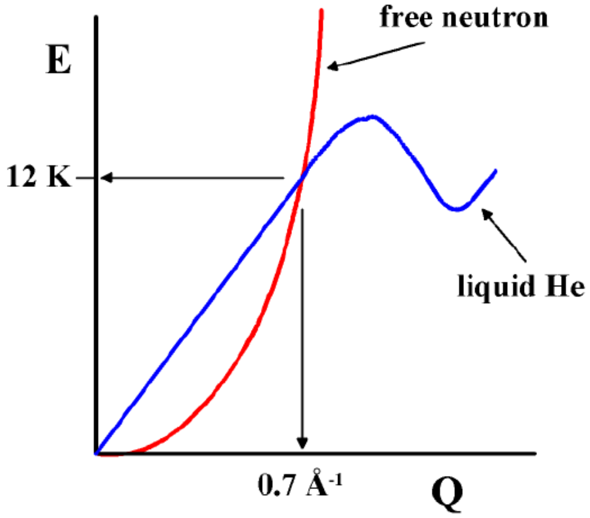

Fig. 1.3. Dispersion laws for a nonrelativistic particle and for superfluid helium.

Figure 1.3 shows dispersion laws (kinetic energy *E* as a function of the momentum transfer *Q*) for a free nonrelativistic particle with mass m ($E = Q^2/2m$) and for the superfluid helium (curve is linear for small *Q* and has a minimum for bigger *Q*). We will not discuss the reason for this *Q*-dependence but we mention only the fact of presence of a crossing point. It means that a neutron with a given momentum *Q* ($0{,}7\,\mathring{A}^{-1}$) can transmit a part of its energy to the superfluid liquid. In this process, a phonon (internal excitation of superfluid helium) is created and neutron loses a part of its velocity. This process is efficient only for neutrons of a given initial energy but it is efficient enough to increase significantly the UCN density, as it was demonstrated in numerous experiments.

The problem is that the UCN are produced inside the superfluid helium and one has to do experiments with these UCN in situ. Their extraction is possible and experimentally proved but the UCN density outside the production volume is not yet very high; these experiments are in progress.

Just to have a more complete vision of different neutron sources, let us mention a new generation of neutron sources developed actively now – neutron spallation sources. These are neutron pulse sources suitable for experiments which do not need a continuum neutron flux.

As an example, one can site new UCN sources called SUNS (Spallation Ultra-cold Neutrons Source) [6] constructed at the PSI (Paul Scherer Institute) in Villigen in Switzerland. An intense proton beam produces neutrons in a lead target. These neutrons are then thermalized in a $4\,m^3$ heavy water volume at room temperature. The UCN are produced in a solid deuterium moderator maintained at very small temperature (~ 6K) and they are then distributed to experiments.

3. Neutron in strong interactions

Neutron is a very important tool to study nuclear interaction in its different manifestations: nucleon-nucleon interactions, nucleon-nucleus interactions, nuclear structure, and nuclear structure of neutron itself. An important part of lectures of this school is devoted to these studies so we'll skip this part but we would like to mention only one point concerning the measurement of nucleon-nucleon scattering length. A very detailed review of this problem can be found in a recent article by Anders Gårdestig [7].

This measurement is a key point to understand isospin (or charge) symmetry as well as its breaking due to electromagnetic interaction and to the different masses of light quarks.

Therefore, precise understanding of nucleon-nucleon (*NN*) interaction is the basis of all nuclear physics. At low energies, this interaction can be described in terms of two phenomenological parameters, scattering length *a* and effective range r_0, defined through so-called effective range expansion of the *S*-wave phase shift $\delta(p)$ as a function of the momentum *p*:

$$p \cot \delta(p) = -\frac{1}{a} + \frac{1}{2} r_0 p^2 + \dots \qquad (3.1)$$

These two phenomenological parameters are practically independent on the nuclear potential shape.

Their currently accepted values corrected theoretically to take into account a difference due to electromagnetic interaction are presented in Table 2. One can see that *nn* and *pp* scattering lengths are close but significantly different.

Table 2. Scattering length *a* and effective range r_0 in *NN* systems.
Electromagnetic effect corrections are theoretically removed.

NN	*a*, fm	r_0, fm
nn	-18.9 ± 0.4	2.75 ± 0.11
np	-23.740 ± 0.020	2.77 ± 0.05
pp	-17.3 ± 0.4	2.85 ± 0.04

One of the main problems here is that our present knowledge of the *nn* scattering length is based exclusively on information obtained from indirect reactions. For instance, the most popular is a study of the deuteron break-up reaction $nd \to nnp$ which has a long, unfortunate history of contradicting results.

This is a reason why there is a strong interest to propose a direct measurement of the nn scattering length. The most serious and advanced proposal is one pursued by the DIANNA collaboration using the pulsed reactor YAGUAR in the former nuclear-weapon city Snezhinsk in Russia [8]. By triggering fusion in a cylindrical reactor containing a uranium salt dissolved in water, the emitted neutrons get moderated by plastic walls as they reach the hollow center of the reactor. Detecting the resulting neutron spectrum, one can determine the *nn* cross section and thus the scattering length. This work is still in progress.

4. Neutron electromagnetic properties

Even being neutral, neutron is characterized by different parameters which reflect its internal electric and magnetic structure. We'll briefly remind these characteristics (charge, form factors, magnetic moment) and we'll spend more time to discuss neutron electric dipole moment – physical phenomenon intensively studied with the UCN since their discovery.

Neutron, by “definition”, is a neutral particle. Its neutrality was verified in a few experiments either by direct measurement of neutron charge or by measurement of neutrality of atoms. The averaged Particles Data Group [9] value for neutron charge is equal to

$$q_n = (-0.2 \pm 0.8) \cdot 10^{-21} e \,. \tag{4.1}$$

Sufficiently more experiments were done to measure neutron charge distribution or neutron electric form factor. As an example, we present here a figure 4.1 taken from [10] which shows neutron electric form factor.

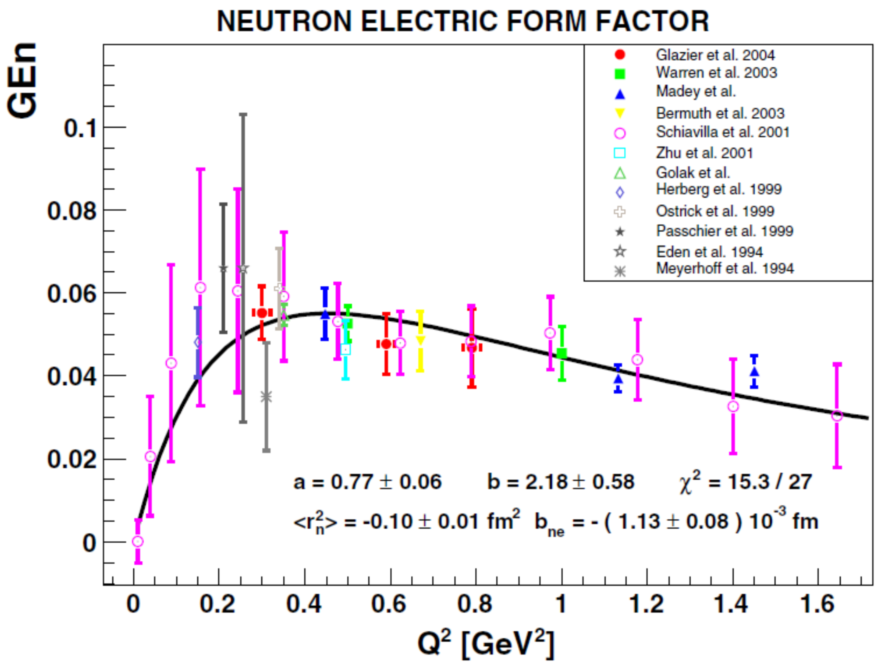

Fig. 3. 1. The neutron form factor $G_E(Q^2)$ as a function of the momentum transferred Q^2.
The experimental data are taken from [11]; the solid curve is a two parameter fit.

The slope of this form factor at zero called the electron-neutron scattering length, which is directly related to the neutron mean-square charge radius and to the neutron electromagnetic form-factor $G_E(Q^2)$ by

$$b_{ne} = -\frac{2}{a_0}\frac{m}{m_e}\frac{dG_E(Q^2)}{dQ^2}\bigg|_{Q^2=0} \,. \tag{4.2}$$

m and m_e being the neutron and electron masses, a_0 the Bohr radius.

Non-zero magnetic moment of neutron is another important property of neutron which allows using this particle as fantastically powerful tool in studies of magnetic properties of different physical, chemical and biological systems. Its value (experimentally known with very high precision) is equal [9]:

$$\mu_n = -(1.91304272 \pm 0.00000045)\mu_B \,.$$

4.1. Neutron electric dipole moment (EDM)

Let us suppose that neutron possesses electric dipole moment which can be described as a product of elementary charge and a distance between positive and negative charges of this dipole:

$$\overrightarrow{d_n} = e \cdot \vec{r} = d_n \hat{\vec{s}} \,. \tag{4.3}$$

The only privileged direction being the neutron spin direction, this vector has to be proportional to spin. The non-zero value of the coefficient of proportionality between these two vectors d_n would mean the parity P violation. One can see it directly from equation (4.3): P-parity changes the sign of the vector $\vec{r} \to -\vec{r}$ but it does not for $\hat{\vec{s}} \to \hat{\vec{s}}$. Therefore the non-zero value of the neutron EDM means P- and T-parity violation as well as CP-violation (if one admits CPT conservation). Today the main motivation to measure the neutron EDM is to search for new physics beyond the Standard Model. The main advantage of this experimental observable with respect to other ones is that, within the Standard Model, the value of neutron EDM is extremely small (~ $10^{-32} \div 10^{-34}\ e \cdot \mathrm{cm}$) and any non-zero value higher than this number would be a manifestation of new physical phenomenon beyond the Standard Model.

Since the first measurement by Ramsey *et al.* [12] done at the end of 50[th], this value was strongly constrained in a long series of more and more sophisticated experiments. The up-to date limit is [13]

$$|d_n| < 2{,}9 \cdot 10^{-26}\ e \cdot \mathrm{cm} \quad (90\%\ \mathrm{CL}) \tag{4.4}$$

This upper limit was established in the experiment done at the ILL. This experiment as well as all other modern experiments aiming to measure neutron EDM uses the Ramsey's method.

In this method, one studies the precession of the spin of UCNs in a combination of magnetic and electric fields. The interaction energy of neutron magnetic moment $\vec{\mu}_n$ with external magnetic field $\vec{B}$, is given by a product $-\vec{\mu}_n \cdot \vec{B}$. In the same way, if neutron has electric dipole moment $\vec{d}_n$ the interaction energy with external electric field $\vec{E}$ is equal to $-\vec{d}_n \cdot \vec{E}$.Total Hamiltonian for these interactions is thus given by:

$$\widehat{H} = -\vec{\mu}_n \cdot \vec{B} - \vec{d}_n \cdot \vec{E}\,. \tag{4.5}$$

And the energy difference between the quantum levels is:

$$\varepsilon = 2\mu_n B \pm 2 d_n E\,. \tag{4.6}$$

Transitions between these levels can be induced by an additional oscillatory magnetic field. This is the general scheme of the Ramsey's method, in which polarized neutrons are injected in to the volume with collinear magnetic and electric fields and one applies a series of oscillatory magnetic field (RF) pulses separated by a period of free precession with duration T. The experimental sequence of these periodic pulses is presented in figure 4.1:

1. Spin of the neutron follows the direction of constant magnetic field (without RF field);
2. One applies a pulse of RF field to put the spin perpendicular to the constant magnetic field;
3. Spin precession around magnetic and electric field axis (with Larmor frequency) during a period T;
4. Additional pulse of RF magnetic field to put neutron spin antiparallel to the magnetic field axis.

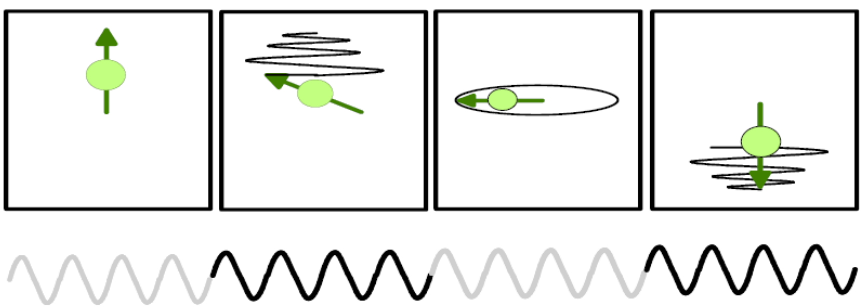

Fig. 4.1. Experimental sequence of the RF magnetic field

The frequency of the spin precession and the phase cumulated depend on the value of the field and define a probability of spin-flip transition (i.e. number of neutrons with opposite spin after the second application of the RF field).

The method consists in a measurement of Larmor resonance frequency and its comparison in for two opposite directions of electric field $\vec{E}$. This frequency difference $\Delta\nu$ is directly proportional to $d_n E$:

$$\Delta\nu = \nu_\uparrow - \nu_\downarrow = \frac{4 d_n E}{h}. \qquad (4.7)$$

One then count a number of neutrons of given polarization for two electric field directions ($\vec{E}\uparrow$ and $\vec{E}\downarrow$) as a function of the RF magnetic field frequency. One example of such a curve is presented in figure 4.2. The fitting procedure give two corresponding frequencies $\nu_\uparrow$ et $\nu_\downarrow$ which allow to determine the upper limit on d_n through equation (4.7).

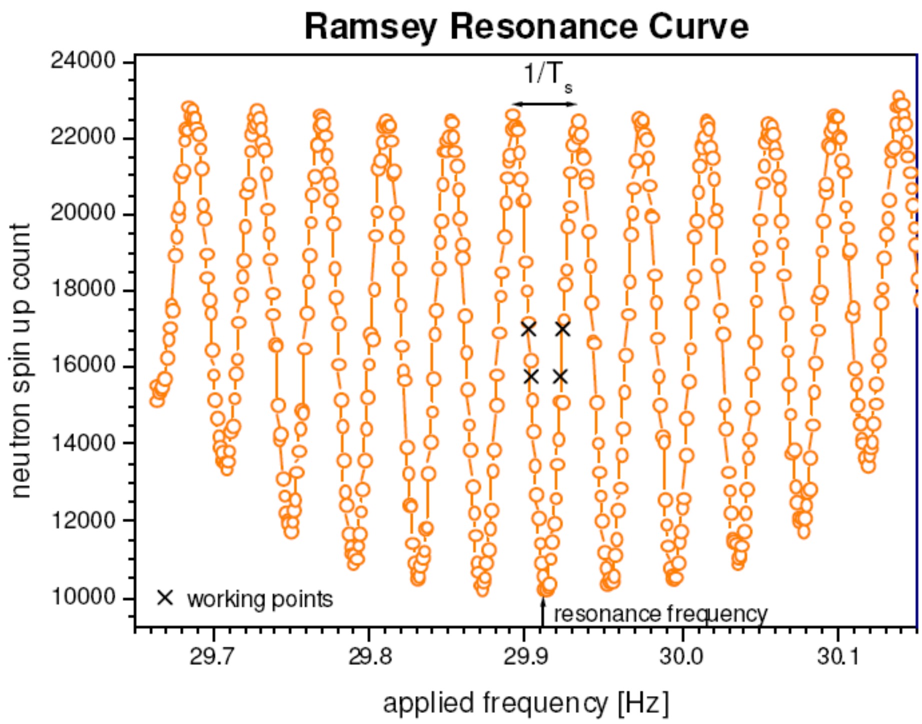

Fig. 4.2. Number of neutrons with spin parallel to constant magnetic field as a function of oscillatory magnetic field frequency (curve de Ramsey).

There a few new project aiming to improve the existing limit on neutron EDM. One of them is under operation with UCN source SUNS at the PSI in Switzerland.

5. Weak interaction

Neuron β-decay $n \rightarrow p + e^- + \bar{\nu}_e$ is an excellent instrument to study weak interaction. This process is very reach in experimental observables and it allows to measure parity-conservations and parity violating effects which are important consequences in particles physics, nuclear astrophysics, Big Bang theory etc. A quite detailed review of these phenomena can be found, for instance, in [14]. In these lectures, we'll mention only one aspect of this reach processes, the neutron life time measurement.

5.1. Neutron life time

One of the most important applications of UCN is the experiment to measure neutron life time τ. Precise measurement of this fundamental constant is very important, at least, for two reasons.

The first one is related to the study of Cabibbo-Kobayashi-Maskawa matrix describing flavor mixing. This matrix should be unitary and this condition implies a relation between the elements describing a coupling between quark *u* and quarks *d*, *s*, and *b*:

$$|V_{ud}|^2 + |V_{us}|^2 + |V_{ub}|^2 = 1. \tag{5.1}$$

This relation should be verified experimentally by direct independent measurement of these three contributions. The first term V_{ud} governs the neutron decay:

$$n \to p + e^- + \bar{\nu}_e \tag{5.2}$$

and it is related to the neutron life time by the relation [9]

$$|V_{ud}|^2 = \frac{(4908,7 \pm 1,9)s}{\tau(1+3\lambda^2)} \tag{5.3}$$

where $\lambda = g_A / g_V$ is ratio of axial-vector and vector weak interaction constants. This ration can be determined with high precision from the asymmetry *A* measured in neutron decay. The error bars in denominator take into account the uncertainty of radiative correction.

The second reason is the role of the neutron life time in the Big Bang Theory. In particular, the primordial nucleosynthesis predicts abundancies of light nuclei (D, ^{3}He, ^{4}He et ^{7}Li) by using different reactions involving neutron ($n \leftrightarrow p + e^- + \bar{\nu}_e$, $n + \nu_e \leftrightarrow p + e^-$, etc.).

There are two main approaches to measure τ: “beam” experiment (studies of in-flight neutron decay) and “bottle” one (decay of UCN stored in material or magnetic trap).

In a beam experiment, on measure the neutron decay rate for a given volume around the beam. The life time is then determined by

$$\frac{dN}{dt} = -\frac{N}{\tau}. \tag{5.4}$$

where *N* is the number of neutrons and dN/dt number of products of decay (protons and electrons) in this volume per time unit. In these experiments, it is necessary to measure precisely both total number of neutrons and decay rate.

In “bottle” experiment, one notes that the solution of equation (5.4) is:

$$N(t) = N(0)\exp\left(-\frac{t}{\tau_{\text{eff}}}\right). \tag{5.5}$$

where we in have introduced explicitly the effective storage time τ_{eff}. This parameter τ_{eff} can be easily determined from two consecutives measurements and it is different from τ due to UCN loses on the walls of the trap volume, characterized by a time τ_{loss}:

$$\frac{1}{\tau_{\text{eff}}} = \frac{1}{\tau} + \frac{1}{\tau_{\text{loss}}}. \tag{5.6}$$

The nature of these losses depends on each concrete experiment. To overcome this difficulty, one uses the fact that these losses are induced by interactions with walls and τ_{loss} should be a function of the ratio of the volume *V* of the trap to its surface *S*. In the limit $V/S \to \infty$ this parameter τ_{loss} should equal to 0. Therefore, the idea is to construct a trap with variable volume and to study the effective storage time as a function of V/S. An extrapolation $\lambda \to \infty$ allows obtaining the neutron life time.

Just to illustrate the situation with τ measured in different experiments, Table 2 presents some results of recent experiments (since 2000) as well as their type (beam or bottle).

Table 2. Neutron life time measured in different experiments.

τ, s	Type	Author, Year
$887.7 \pm 1.2 \pm 1.9$	beam (reanalysis 2005)	A.T. Yue et al. *Phys. Rev. Lett.* **111** (2013) 222501
$881.6 \pm 0.8 \pm 1.9$	bottle (reanalysis 2000)	S.S. Arzumanov et al. *JETPLett*. **95** (2012) 224
$882.5 \pm 1.4 \pm 1.5$	bottle (reanalysis 1989)	A. Steyerl et al. *Phys. Rev*. **C85** (2012) 065503
$880.7 \pm 1.3 \pm 1.2$	bottle	A. Pichlmaier et al. *Phys. Lett*. **B693** (2010) 221
$878.5 \pm 0.7 \pm 0.3$	bottle	A.P. Serebrov et al. *Phys. Lett*. **B605** (2005) 72
$886.3 \pm 1.2 \pm 3.2$	beam	J.S. Nico et al. *Phys. Rev*. **C71** (2005) 055502
$885.4 \pm 0.9 \pm 0.4$	bottle	S.S. Arzumanov et al. *Phys. Lett*. **B483** (2000) 15

There are still quite important discrepancies in these experimental results and recent active reanalysis of experimental data shows the necessity to find the origin of these discrepancies. Anyway, the world averaged value of the neutron life time calculated by the PDG group is equal to [9]

$$\tau = (880,0 \pm 0,9)\ \text{s}. \tag{5.7}$$

6. Neutron in gravity field

Pioneering studies of neutron behavior in gravity field starts in middle of 70th by a very elegant and sophisticated experiment of neutron interferometry, performed by Collela, Overhauser, and Werner [15]. This experiment allowed, in particular, to compare neutron inertial and gravitational mass.

But an intensive study of this interaction with neutrons starts from the discovery of neutron quantum states in gravity field done fifteen years ago [16–18]. In these lectures, we'll present only these experiments.

The problem of motion of a particle in a linear potential above an infinite well is a very good quantum mechanics exercise known since very long date and can be found in most of good text books. For a long time, this problem was considered only as a good theoretical exercise in quantum mechanics. The main obstacle for observing these quantum states experimentally was the extreme weakness of the gravitational interaction with respect to electromagnetic one, which meant that the latter could produce considerable false effects. In order to overcome this difficulty, an electrically neutral long-life particle (or quantum system) must be used for which an interaction with a mirror can be considered as an ideal total reflection. The experimental observation of these states become possible only quite recently with the UCN at the ILL .

Let us remind briefly the solution of this quantum mechanical problem [19]. The wave function $\psi(z)$ of the neutron in the Earth's gravitational field above an ideal mirror ($z > 0$) satisfies the Schrödinger equation:

$$\frac{\hbar^2}{2m}\frac{d^2\psi(z)}{d^2z} + (E - V(z))\psi(z) = 0. \tag{6.1}$$

An ideal mirror at $z = 0$ could be approximated as an infinitely high and sharp potential step (infinite potential well):

$$V(z)=\begin{cases}\infty, & z<0\\ mgz, & z>0\end{cases}. \tag{6.2}$$

Note that the neutron energy in the lowest quantum state, as will be seen a little later, is of the order of 10^{-12} eV and is much lower than the effective Fermi potential of a mirror, which is close to 10^{-7} eV. The range of increase of this effective potential does not exceed a few nm, which is much shorter than the neutron wavelength in the lowest quantum state ~10 μm. This effective infinite potential gives a zero boundary condition for the wave function:

$$\psi(z=0)=0. \tag{6.3}$$

The exact analytical solution of equation (2.15) which is regular at $z=0$, is the so-called Airy-function [20]:

$$\psi(z)=C\,\mathrm{Ai}\left(\frac{z}{z_0}\right). \tag{6.4}$$

Here,

$$z_0=\sqrt[3]{\frac{\hbar^2}{2m^2g}}\approx 5.87\ \mu\mathrm{m} \tag{6.6}$$

represents a characteristic scale of the problem, C being the normalization constant. The equation (6.3) imposes the quantization condition:

$$z_n=z_0\lambda_n, \tag{6.7}$$

where λ_n are zeros of the Airy function. They define the quantum energies:

$$E_n=mgz_0\lambda_n. \tag{6.8}$$

For the first four quantum states, on obtains

$$\lambda_n=\{2.34,\ 4.09,\ 5.52,\ 6.79,\ \ldots\} \tag{6.9}$$

and

$$E_n=\{1.4,\ 2.5,\ 3.3,\ 4.1,\ \ldots\}\ \mathrm{peV}. \tag{6.10}$$

Formally, these functions do not equal zero at any height $z>0$. However, as soon as a height z is greater than some critical value z_n, specific for every n-th quantum state and approximately equal to the height of the neutron classical turning point, then the probability of observing a neutron approaches zero exponentially fast. Such a pure quantum effect of the penetration of neutrons to a classically forbidden region is well-known tunneling effect.

Such a wave-function shape allowed us to propose a method for observing the neutron quantum states. The idea is to measure the neutron transmission through a narrow slit Δz between a horizontal mirror on the bottom and a scatterer/absorber on top (which we shall refer to simply as a scatterer if not explicitly called otherwise). If the scatterer is much higher than the turning point for the corresponding quantum state, then neutrons pass such a slit without significant losses. When the slit decreases, the neutron wave function $\psi_n(z)$ starts penetrating up to the scatterer and the probability of neutron losses increases. If the slit size is smaller than the characteristic size of the neutron wave function in the lowest quantum state, then such a slit is not transparent for neutrons.

A basic scheme of this experiment is presented in figure 6.1. The experiment consists of measuring of the neutron flux (with an average velocity of 5–10 m/s) through a slit between a mirror and a scatterer as a function of the slit size. The size of the slit between the mirror and the scatterer can be finely adjusted and precisely measured. The scatterer's surface, while macroscopically smooth and flat, is microscopically rough, with roughness elements measuring in microns. In the classical approximation, one can imagine that this scatterer eliminates those neutrons whose vertical velocity component is sufficient for them to reach its surface. Roughness elements on the scatterer's surface lead to the diffusive (non-specular) reflection of neutrons and, as a result, to the mixing of the vertical and horizontal velocity components. Because the horizontal component of the neutron velocity in our experiment greatly exceeds its vertical component, such mixing leads to multiple successive impacts of neutrons on the scatterer/absorber and, as a result, to the rapid loss of the scattered neutrons.

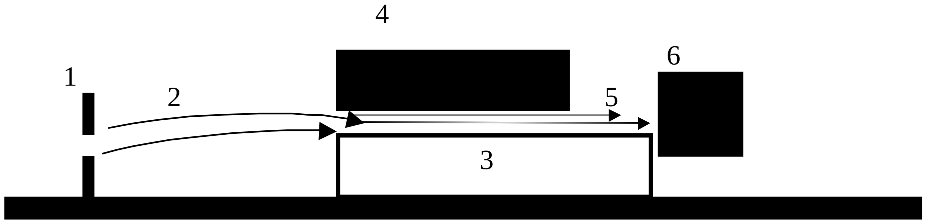

Fig. 6.1. A basic scheme of the first experiment. From left to right: the vertical bold lines indicate the upper and lower plates of the input collimator (1); the solid arrows correspond to classical neutron trajectories (2) between the input collimator and the entrance slit between the mirror (3, the empty rectangle below) and the scatterer (4, the black rectangle above). The dotted horizontal arrows illustrate the quantum motion of neutrons above the mirror (5), and the black box represents a neutron detector (6). The size of the slit between the mirror and the scatterer could be changed and measured.

The results of the measurement presented in figure 6.2 [17, 18] differ considerably from the classical dependence and agree well with the quantum-mechanical prediction. In particular, it is firmly established that the slit between the mirror and the scatterer is opaque if the slit is narrower than the spatial extent of the lowest quantum state, which is approximately 15 μm. The dashed line in figure 6.2 shows the results of a quantum-mechanical calculation, in which the level populations and the height (energy) resolution were treated as free parameters. The solid line shows the classical dependence normalized so that, at sufficiently large heights, the experimental results are described well by the line. The dotted line given for illustrative purposes describes a simplified situation with the lowest quantum state alone, i.e. in drawing this line only the uncertainty relation was taken into account. As can be seen from figure 6.2, the statistics and energy resolution of the measurements are still not good enough to detect quantum levels at a wide slit, but the presence of the lowest quantum state is clearly revealed.

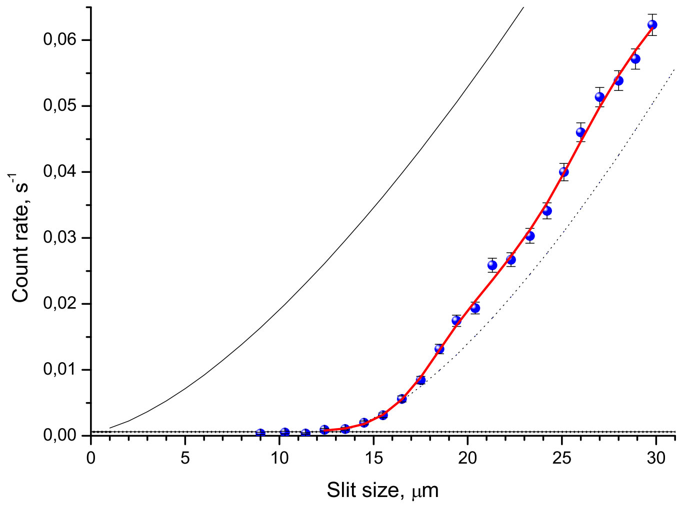

Fig. 6.2. Neutron flux through a slit between a horizontal mirror and a scatterer above it is given as a function of the distance between them obtained in the second experiment [17].

In order to resolve higher quantum states clearly and measure their parameters accurately, we must adopt other methods, such as for example, the "differential" method, which uses position-sensitive neutron detectors with a very high spatial resolution, which were developed specifically for this particular task [21]. Clearly, the differential technique is much more sensitive than the integral one and makes it possible to gain the desired statistical accuracy much faster. This is of prime importance considering the extremely low counting rate in this experiment, even with the use of the highest UCN flux available today. Furthermore, the scatterer employed in the integral technique inevitably distorts the measured quantum states by deforming their eigen-functions and shifting their energy values. The finite accuracy of taking these distortions into account results in systematic errors and ultimately limits the attainable accuracy of the measurement of the quantum state parameters. For these and other reasons, the use of a position-sensitive detector to directly measure the probability of neutron residence above the mirror is highly attractive. However, until now there were no neutron detectors with the spatial resolution of ~1 μm needed for this experiment. We therefore had to develop such a detector and measuring technique. The result was a plastic track nuclear detector (CR39) with a thin uranium coating ($^{235}UF_4$), described in ref. [21]. The tracks created by the entry into the plastic detector of a daughter nucleus produced by the neutron-induced fission of a ^{235}U nucleus were increased to ~1 μm in diameter by means of chemical development. The developed detector was scanned with an optical microscope over a length of several centimeters with an accuracy of ~1 μm. The measuring technique and the preliminary analysis of the results are described in ref. [15].

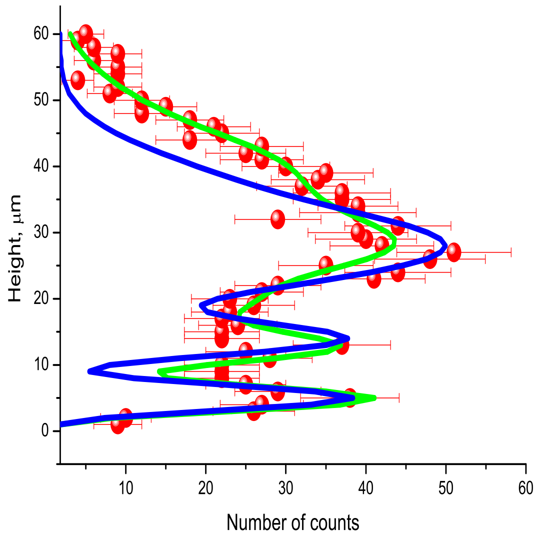

Fig. 2.11. The neutron density distribution in the gravitational field is measured using position-sensitive detectors of extra-high spatial resolution. The circles indicate experimental results. The blue curve corresponds to the theoretical expectation under the assumption of an ideally efficient scatterer able to select a single quantum state above the mirror (1) and no parasitic transitions between the quantum states above the mirror (2). The green curve corresponds to the more realistic fit using precise wave-functions and free values for the quantum states populations.

7. Search for additional interactions

As we saw in these lectures, neutron is a perfect and rare elementary particle to study all known fundamental interaction: strong, weak, electromagnetic, and gravitational. Moreover, it appears to be a very powerful tool to search for other hypothetical interactions. A review of these studies for spin-independent and spin-dependent forces can be found in [10, 22, 23].

The existence of other fundamental interactions in nature, mediated by new bosons, has been extensively discussed, given their possibility in many extensions of the Standard Model of particle physics [24–30]. For instance, theories with large extra spatial dimensions provide strong motivation to search for such forces. If a boson is allowed to travel in large extra compactified dimensions, with a strong coupling constant in the bulk, it behaves in our 4d world as a very weakly coupled new boson, the coupling being diluted in the extra dimensions. The light dark matter hypothesis also argues in favor of the existence of new short range interactions. New bosons, for example, are predicted by most of the grand unified theories embedding the Standard Model, with the coupling constant of ~0.1. These strongly coupled bosons have to be heavier than ~1 TeV if they were not to conflict with present observations; heavier bosons will be searched for at the Large Hadron Collider. Lighter bosons could mediate a finite range interaction between two fermions:

$$V(r) = Q_1 Q_2 \frac{g^2}{4\pi} \frac{\hbar c}{r} e^{-r/\lambda} \tag{7.1}$$

where *V(r)* is the interaction potential, *g* is the coupling constant, Q_1 and Q_2 are the charges of the fermions under the new interaction, and the range of this Yukawa-like potential $\lambda = \hbar / Mc$ is inversely proportional to the boson mass *M*. We consider the interactions of neutrons with nuclei of atomic number A, thus the charge of the atom under the new interaction is equal $Q_1 = A$, and the neutron charge is equal to unity $Q_2 = 1$. The presence of light bosons would be shown by deviations from the gravitational inverse square law.
For instance, the scattering of slow neutrons on atoms is described by the scattering amplitude $f(\mathbf{q})$; this can be represented by a sum of a few terms [31]:

$$f(\mathbf{q}) = f_{\text{nucl}}(\mathbf{q}) + f_{ne}(\mathbf{q}) + f_V(\mathbf{q})\,. \tag{7.2}$$

The first, the most important term, represents the scattering due to the nuclear neutron-nucleus interaction. At low energies discussed in these lectures, it is isotropic and energy independent, because the nuclear radius is much smaller than the wavelength of slow neutrons:

$$f_{\text{nucl}}(\mathbf{q}) = -b\,. \tag{7.3}$$

The coherent scattering length *b* is the fundamental parameter describing the interaction of slow neutrons with a nucleus.
The second term is the amplitude of so-called electron-neutron scattering due to the interaction of the neutron charge distribution with the nucleus charge and the electron cloud. This amplitude can be written as

$$f_{ne}(\mathbf{q}) = -b_{ne}\left(Z - f(Z,\mathbf{q})\right) \tag{7.4}$$

with $f(Z,\mathbf{q})$ is the atomic form-factor measured in the X-rays experiments and b_{ne} already introduced in equation (4.2).
In the presence of a new interaction (7.1), the scattering due to the extra interaction, within the Born approximation, is given by

$$f_V(\mathbf{q}) = -A\frac{g^2}{4\pi}\frac{c}{\hbar}\frac{2m\lambda^2}{1+\left(q\lambda\right)^2}\,. \tag{7.5}$$

As an example, in figure 7.1 taken from [10], we present some constraints on the hypothetical interaction (7.1) which can be obtained from different experiments done with neutrons.

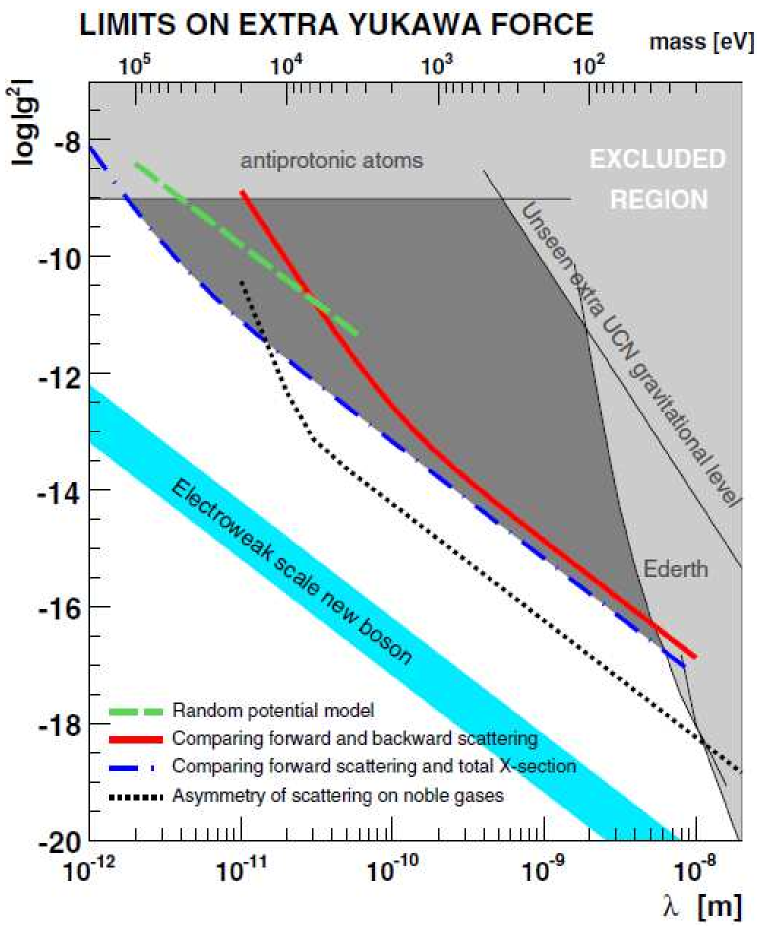

Fig. 7.1. The shaded regions correspond to current experimental limits on extra Yukawa interaction. It includes constraint at 95% C.L. (dashed, dot-dashed, and bold lines) obtained in this article, and the existing constraints. The dotted line is an estimation of the sensitivity of the proposed experiment.

8. Neutron whispering gallery

To improve these limits, one needs to find other physical systems where neutron behavior can be described very precisely and where one can search for a deviation from this known and good understood behavior. Such a news system proposed less than ten years ago is so-called neutron whispering gallery where one studies the motion of a neutron along the board of a cylinder.

Neutron localization in the ‘centrifugal states’ near a curved mirror surface [32–34] is a quantum analogue of the so-called whispering gallery wave. The whispering gallery effect has been known in acoustics since ancient times and was explained by Lord Rayleigh in his Theory of Sound [35]. This phenomenon in optics has been the object of growing interest during the last decade due to their multiple applications. In the following, we will be interested in the matter–wave aspect of the whispering gallery wave phenomenon: namely, large-angle neutron scattering on a curved mirror. Such a scattering can be understood in terms of the states of a quantum particle above a mirror in a linear potential, in analogy to the neutron quantum motion in the Earth’s gravitational field above a flat mirror presented here in chapter 6.

The observed phenomenon consists of the localization of cold neutrons near a curved mirror surface due to the superposition of the centrifugal potential and optical potential of the mirror. In this case, the centrifugal states play an essential role in the neutron flux dynamics.

Measurement of the gravitationally bound and centrifugal quantum states of neutrons could be considered as a direct confirmation of the Weak Equivalence Principle for a massive particle in a quantum state discussed above. Evident advantages of using cold neutrons (neutrons of a thousand meter per second velocity) instead of UCNs include much higher statistics being attainable, broad accessibility of cold neutron beams.
For the first time, the neutron scattering on a curved mirror was studied in [32] and their detailed description was done in [34]. If the neutron energy is much larger than the mirror optical potential, most neutrons scatter to small angles. However, some neutrons could be captured into long-living centrifugal quasi stationary states localized near the well-polished curved surface of the mirror and thus could deflect to large angles. The curved mirror surface plays the role of a waveguide and the centrifugal states play the role of radial modes in such a waveguide schematically presented in figure 8.1.
The quantum well is formed by the effective centrifugal potential and the repulsive optical potential of a curved mirror as shown in figures 8.1 and 8.2. The effective acceleration near the curved mirror surface could be approximated by $a = v^2 / R$, where v is the neutron velocity and R is the mirror radius.

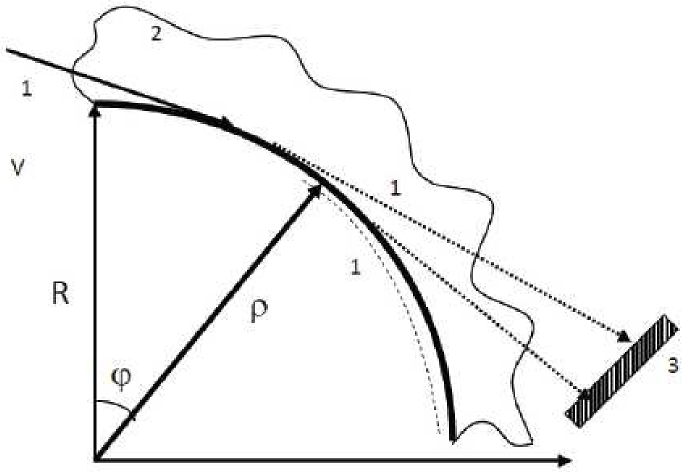

Fig. 8.1. A scheme of the neutron centrifugal experiment. 1: classical trajectories of incoming and outcoming neutrons, 2: cylindrical mirror, 3: neutron detector, 4: quantum motion along the mirror surface.

If we vary continuously the longitudinal velocity v (i.e. the neutron wavelength λ), we change the width of the triangular barrier, thus changing the number of quasistationary states that can propagate along the mirror. It is important that below some critical wavelength λ_c no quasistationary states with sufficiently long lifetimes can be formed, so the neutron scattering probability to large angles is expected to have a sharp cut-off below λ_c.With increasing neutron wavelength λ the number of states increases, resulting in interference maxima and minima in the scattering probability.
To describe this experimental system, one can start from the scattering on the cylinder (two dimensional potential well of the depth U_0) of radius R:

$$U(\rho) = \begin{cases} -U_0, & \rho < R \\ 0, & \rho > R \end{cases}. \qquad (8.1)$$

The solution of the Schrodinger equation $\Phi(\rho,\varphi)$ can be developed as

$$\Phi(\rho,\varphi) = \sum_{m=-\infty}^{+\infty} \chi_m(\rho) e^{im\varphi} . \qquad (8.2)$$

The radial wave function obeys the equation ($\hbar = 1$)

$$\left[-\frac{1}{2M}\frac{d^2}{d\rho^2}+\frac{1}{2M\rho^2}\left(m^2-\frac{1}{4}\right)-U(\rho)-\frac{p^2}{2M}\right]\chi_m(\rho)=0\,. \tag{8.3}$$

with regular boundary condition at the origin and usual asymptotic behaviour.

$$\begin{aligned}&\chi_m(\rho\to 0)=0,\\&\chi_m(\rho\to\infty)=\sqrt{\frac{2}{\pi p}}\sin\left(p\rho+\delta_m-\frac{\pi}{2}\left(|\mu|-\frac{1}{2}\right)\right),\end{aligned} \tag{8.4}$$

$\delta_m(p)$ is the scattering phase.

It is easy to note that these equations coincide with the usual equations used in the Regge formalism [36]. This fact allows using the corresponding method of complex angular momentum in which the scattering amplitude

$$f(p,\varphi)=\sum_{m=-\infty}^{+\infty} f(m,p)e^{im\varphi}\to\frac{1}{i}\sqrt{\frac{1}{2\pi p}}\int_{-\infty}^{+\infty}\left(e^{2i\delta_m(p)}-1\right)e^{im\varphi}dm\,. \tag{8.5}$$

Is calculated as a sum of partial amplitudes $f(m,p)$ considered as a function of complex momentum μ. This function $f(\mu,p)$ coincides with the scattering matrix for integer values of $\mu=m$ and has standard analytical properties in the complex plane of μ [36, 37]. The sum (8.5) over integer μ is then transformed to an integral in the complex μ plane, which is calculated by using the residue theorem and is replaced by a sum over poles contributions:

$$f(p,\varphi)\to\sqrt{\frac{2\pi}{p}}\sum_i \mathrm{Res}\, e^{2i\delta_{\mu_i}(p)}e^{i\,\mathrm{Re}\,\mu_i\varphi}e^{-\mathrm{Im}\,\mu_i\varphi}+\ldots \tag{8.6}$$

$\mathrm{Res}\, e^{2i\delta_{\mu_i}(p)}$ is a residue of the amplitude in the mentioned pole.

The physical sense of the above expressions for the scattering amplitude is transparent. The corresponding amplitude is the sum of the contributions of decaying neutron quasi-stationary states (each corresponds to the *S*-matrix pole), which are formed during the neutron scattering on the cylinder. The neutron states with the longest lifetime determine the neutron scattering to the large angles. In the following, we will show that such long-living states are the states localized near the cylinder surface and corresponding to the whispering gallery waves.

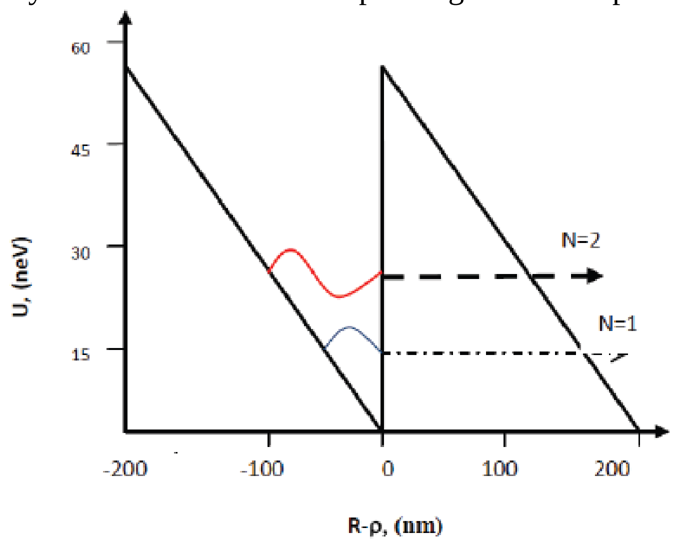

Fig. 8.2. A sketch of the potential in the mirror surface vicinity is shown. The potential step at $z = 0$ is equal to the mirror optical potential. The potential slope at $z = 0$ is governed by the centrifugal effective acceleration $a = v^2 / R$.

In order to solve the equation given above, we expand the expression for the centrifugal energy in equation (8.3) in the vicinity of $\rho = R$ introducing the deviation from the cylinder surface $z = \rho - R$. In the first order of small ratio z / R, we obtain the Schrödinger equation with a linear potential (see figure 8.2) for which the solutions are very close to those obtained for gravitational potential.
The quantum quasistationary states are localized within an effective well, formed by the centrifugal potential and a mirror optical potential. Their properties were studied in details in [33, 34]. The interference picture produced by these quantum states (experimental data and theoretical calculation) is presented in figure 8.3.

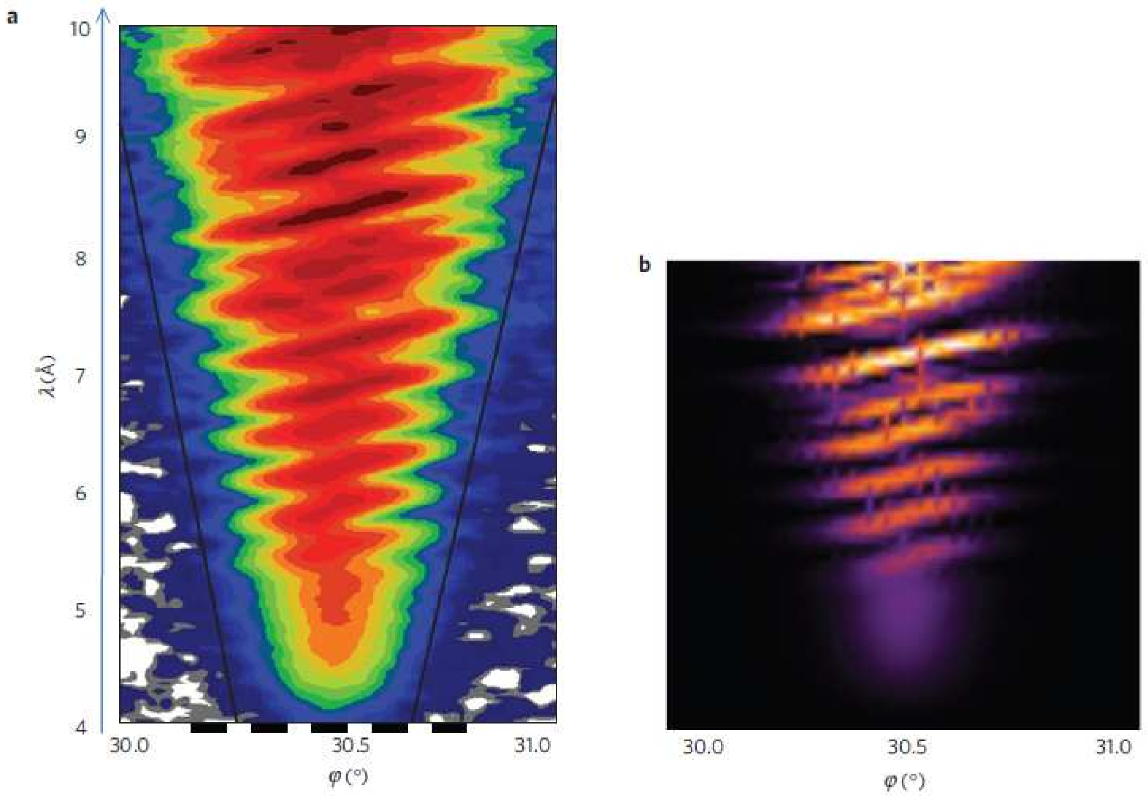

Fig. 8.3. The scattering probability as a function of neutron wavelength λ (vertical axis) and deviation angle φ horizontal axis).

The complex angular momentum method allows us also to give another vision to the problem and to establish more clear analogies with another extensively studied case, that is, scattering of light by a sphere and, in particular, useful similarities with phenomena of rainbow, Gloria, surface waves, and so forth, treated in detail in a book by Nussenzweig [38].
This phenomenon could provide a promising tool for studying fundamental neutron-matter interactions, as well as surface physics effects. Compared with experiments at standard reflectometers using a single reflection, the centrifugal quantum states have the advantage of at least a few hundred or thousand quasi-classical reflections, providing an extremely high sensitivity to the shape of the bounding potential.

By way of conclusion of these lectures, we would like to emphasize once more that the neutron is a fantastic particle involved in a lot of interesting physical problems. The new generation experiments and installations coming in operation would give a new impetus to this fascinating physics.

References

[1] R. Golub, D.J. Richardson, S.K. Lamoreux, *Ultracold Neutrons*; Higler: Bristol, 1991.

[2] V.K. Ignatovich, *The Physics of Ultracold Neutrons*; Clarendon: Oxford, 1990.

[3] V.I. Luschikov, Yu.N. Pokotilovsky, A.V. Strelkov, F.L. Shapiro, *JETP Lett.*, **9** (1969)40.

[4] A. Steyerl, *Phys. Lett.* **B29** (1969) 33.

[5] R. Golub, J.M. Pendlebury, *Phys. Lett.* **A53** (1975) 133.

[6] http://ucn.web.psi.ch/index.htm

[7] A. Gårdestig, *J. Phys. G: Nucl. Part. Phys.* **36** (2009) 053001.

[8] W.I. Furman et al., *J. Phys. G: Nucl. Part. Phys*. **28** (2002) 2627;
G. E. Mitchell et al., *J. Res. Natl. Inst. Stand. Technol*. **110** (2005) 225;
A.Yu. Muzichka et al., *Nucl. Phys*. **A789** (2007) 30.

[9] K.A. Olive et al. (Particle Data Group), *Chin. Phys*. **C38** (2014) 090001 (http://pdg.lbl.gov).

[10] V.V. Nesvizhevsky, G. Pignol, K.V. Protasov, *Phys. Rev*. **D77** (2008) 034020.

[11] http://www.jlab.org/~cseely/formfactor_data.txt

[12] J.H. Smith, E.M. Purcell, N.F. Ramsey, *Phys. Rev*. **108** (1975) 120.

[13] C.A. Baker et al., *Phys. Rev. Lett.* **97** (2006) 131801.

[14] J. Byrne, *An Overview Of Neutron Decay*, in Proceedings of Proceedings of the two day workshop Quark-Mixing, CKM-Unitarity Heidelberg, Germany 19 to 20 September 2002, Edited by Hartmut Abele and Daniela Mund, p. 15.

[15] R. Collela, A.W. Overhauser, S.A.Werner, *Phys. Rev. Lett.* **34** (1975) 1472.

[16] V.V. Nesvizhevsky et al., *Nature* 2002, **415**, 297.

[17] V.V. Nesvizhevsky et al., *Phys. Rev*. 2003, **D67**, 102002-1.
V.V. Nesvizhevsky et al., *Phys. Rev*. 2003, **D68**, 108702.

[18] V.V. Nesvizhevsky et al., *Eur. Phys. J.* 2005, **C40**, 479.

[19] S. Flügge, *Practical Quantum Mechanics*; Springer-Verlag: Berlin, 1974; Vol. 1.

[20] L.D. Landau, E.M. Lifshits, *Quantum Mechanics*; Pergamon Press: Oxford, 1977.

[21] V.V. Nesvizhevsky et al., *Nucl. Instr. and Meth. in Phys. Res.* **A440**, (2000) 754.

[22] S. Baeßler et al, *Phys. Rev*. **D75** (2008) 075006.

[23] I. Antoniadis, et al., *Short-range fundamental forces*. Proc. of the Workshop GRANIT-2010, 14-19 February 2010, Les Houches, France, *Comp. Rend. Phys.* **12** (2011) 755.

[24] I. Antoniadis, *Phys. Lett*. **B246** (1990) 377.

[25] J.D. Lykken, *Phys. Rev*. **D54** (1996) R3693.

[26] *N. Arkani-Hamed et al*., *Phys. Lett*. **B429** (1998) 263.

[27] I. Antoniadis, et al., *Phys. Lett*. **B436** (1998) 257.

[28] V.A. Rubakov et al., *Phys. Lett*. **B125** (136) (1983) 139.

[29] M. Visser, *Phys. Lett*. **B159** (1985) 22.

[30] A. Frank et al., *Phys. Lett*. **B582** (2004) 15.

[31] V. F. Sears, *Phys. Rep*. **141** (1986) 281.

[32] V.V. Nesvizhevsky et al., *Nature Phys*. **6** (2010) 114.

[33] V.V. Nesvizhevsky et al., *Phys. Rev*. **A78** (2008) 033616.

[34] R. Cubitt et al, *New J. Phys*. **12** (2010) 113050.

[35] Strutt Baron Rayleigh J W, 1878, *The Theory of Sound*, vol 2 (London: Macmillan);
L.Rayleigh, *Phil. Mag*. **27** (1914) 100.

[36] H.M. Nussenzweig, 1972, *Causality and Dispersion Relations* (New York: Academic)

[37] V. De Alfaro and T. Regge, 1965, *Potential Scattering* (Amsterdam: North-Holland)

[38] H.M. Nussenzweig, *Diffraction Effects in Semiclassical Scattering*, Cambridge University Press, 1992.